

Interfacial debonding detection in bonded repair with acoustic-optical technique

*XU Ying¹⁾, YaQi Li²⁾

¹⁾ *ShenZhen Key Lab of Urban & Civil Engineering Disaster Prevention & Reduction, Harbin Institute of Technology Shenzhen Graduate School, Shenzhen 518055, China*

²⁾ *School of Electronic and Information Engineering, Shenzhen Polytechnic, Shenzhen*

¹⁾ cexyx@hotmail.com

²⁾ leeyaqi@163.com

ABSTRACT

Based on free vibration theory of a thin plate, an acoustic-optical fiber NDE technique is proposed for the detection of interfacial debonding in bonded repair. A focused sound beam generated from variable frequency loudspeaker source can be controlled to form a local vibration field at the surface of a FRP-retrofitted structure. Local vibration anomalies caused by interfacial debonding in the structure can be measured by surface-mounted optical fiber interferometer, and thus, interfacial debonding can be detected, mapped, and quantified. Based on the results from both numerical and experimental studies, the feasibility of interfacial debonding detection in bonded repair with the proposed technique is demonstrated.

Keywords

FRP; interfacial debonding; optical fiber interferometer; focused sound beam; finite element method

1. Introduction

With the recent development of high strength fibers and adhesives, the adhesive bonding of fiber composite patches has become a popular methodology for structural repair. For example, repair with fiber-reinforced plastic (FRP) plate, which is simple and effective, has been performed on various structures built with concrete [1-4]. Compared to steel, fiber-reinforced plastic plates offer higher ratio of strength to weight and improved durability [5]. For the repair to be effective, the bonded plate must work together with the original structure. However, under variable conditions,

1) Associate Professor

2) Assistant Professor

interfacial debonding of the bonded plate from the substrate may occur. Debonding may initiate at the end of the bonded plate, where a high strain gradient exists [6,7]. When the workmanship is not good enough, imperfect bonding may lead to the formation of debonded zones under the plate [8]. Debonding may also initiate at the bottom of a flexural crack, leading to the formation of a debonded region away from the edge of the plate [9]. If debonding is left unnoticed, its continual growth will lead to failure of the repair [10, 11]. The detection of the interfacial debonding in its early stage is hence a very important task in monitoring the health of structures retrofitted with bonded plates. There are many conventional nondestructive testing methods for interfacial debonding detection in bonded repair, such as ultrasonic technique, X-ray technology, acoustic emission technology and infrared detection technology[4]. The principle of ultrasonic technique is that the elastic waves spreading among solids may introduce reflected waves in case of encountering the inhomogeneous medium and the defects or cracks inside the objects can then be detected. The disadvantage of this technique is that the FRP plate itself is inhomogeneous medium and it is not easy to detect the debonding conditions of interface with ultrasonic waves [5,6]. For X-ray technique, the location and size of stripping layer is detected by measuring power loss. However, the operating cost of X-ray technique is relatively high and only point-by-point detection can be performed with low efficiency. Furthermore, the operating technician can easily be hurt by radiation. It is therefore seldom applied in the practical nondestructive testing project [5]. Also known as stress-wave emission technique, acoustic emission technique acts as a kind of means for nondestructive testing and nondestructive evaluation. This technique adopts high-sensitivity sensors to receive acoustic emission signals transmitted from the occurrence or extension of defects and damages when materials or components bear external force before they are far from being damaged. By analyzing and disposing these signals, the internal characteristics on these defects and damages for materials and components are detected and evaluated [5-7]. The disadvantage of this method is that the received waves can be easily affected by noise so that the accuracy of detected result cannot be guaranteed. In addition, acoustic emission detection has to be carried out under specific loading conditions. At present, only location, activity, and strength of acoustic emission source can be provided while the character and size of defects of acoustic emission source cannot be accurately provided. Infrared detection technique takes advantage of change of heat conduction mode of object in case that cracks or defects exist, thus the discrepancy or uneven changes of infrared radiation on the object surface will appear. By detecting these discrepancy or uneven change, the location and size of defects can be intuitively found out [2,6]. By adopting this method, the damage location can be approximately determined; however, due to boundary ambiguity problem for infrared detection method, it is hard to measure the dimension of interfacial debonding for FRP retrofitted structure quantitatively.

In general, most conventional nondestructive testing methods have disadvantages such as expensiveness, low sensitivity and absence of real-time control. In addition, the excitation actuator is generally required to be tested near the structure surface (semi-contact type), on the surface or embedded inside the structure (contact-type). With the increasing use of FRP-strengthening in various engineering structures, it is of growing importance to develop reliable, effective, and non-contact nondestructive evaluation methods to assess and monitor the mechanical serviceability and safety of in-service FRP-retrofitted structures. Focused acoustic beam can be used as non-contact excitation actuator to excite the FRP-concrete system from ranges exceeding 10 meters. Therefore, a powerful loudspeaker source which drives a linear chirp is utilized to generate focused sound beam such that the beam diameter can be controlled to directly and locally excite the surface area where damages/defects are embedded in the FRP-concrete systems. A pre-attached high-sensitivity fiber optic interferometer is used to detect the local micro vibration of the FRP reinforced structure surface caused by the acoustic excitation. Hence, by analyzing the vibration characteristics the location and size of debonding damage can be detected.

2. The detection principle

The basic principle for the detection of interfacial debonding damage in FRP-retrofitted structures using acoustic-optical fiber is shown in Figure 1. The loudspeaker which drives a linear chirp (eg. 50Hz~2KHz) generates acoustic wave to locally excite the surface area of FRP-retrofitted structure, and the vibration in this local area and at the nearby area may form into a vibration field. When debonding occurs at the interface of FRP-retrofitted structures, hole or cavity will be created in the debonding zone. If the cross-section shape of the interface debonding is simplified as a circle, the FRP sheet located above the hole or cavity can be treated as circular thin plate with fixed edge supports. The vibration of the thin plate at fundamental natural frequency can be obtained by analytical solution. When the focused sound beam excites the surface area where debonding is embedded in the FRP-concrete systems, one of the frequency component of the loudspeaker source may be close to or equal to the fundamental natural frequency of the thin FRP plate located above the debonding zone. Therefore, high velocity measurements can be observed at the debonding location and at the resonant frequency relating to the defect geometry. Regarding that the acoustic beam energy is limited, the acoustically excited vibration of FRP sheet surface is relatively weak. These vibration anomalies can be measured at the target surface using a pre-attached high-sensitivity fiber optic interferometer, and thus, interfacial debonding can be detected, mapped, and quantified.

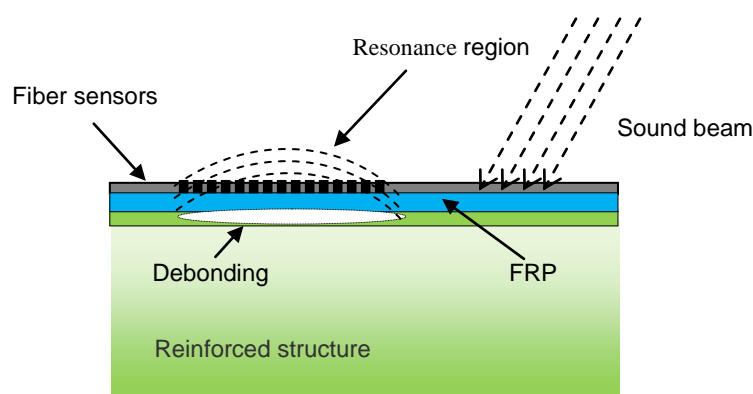


Figure1 The principle of interfacial debonding detection for FRP-retrofitted structures with variable-frequency sound beam

3. Numerical Analysis

3.1 Finite Element Model

The commercial software ABAQUS was adopted to simulate the surface vibration of FRP-retrofitted structure with interfacial debonding under the acoustic waves generated by loudspeaker with linear frequency conversion. FRP-retrofitted concrete panels and beams with different debonding shapes were considered in this study. For FRP-retrofitted concrete panels, the debondings are located at the midspan with circular shape. For FRP-retrofitted concrete beams, the debondings are either located at the midspan with circular or rhombic shape or located near the edge of the FRP plate with rectangular shape. The debonding with circular shape was utilized to simulate interfacial defect or bubble with irregular shapes, the debonding with rhombic shape was utilized to simulate debonding damage in the middle of components, and the debonding with rectangular shape was utilized to simulate debonding near FRP plate edge. The thickness of FRP plate and adhesive are both 0.3mm. The material properties of FRP sheet and substrate concrete are listed in Table 1. Elements SOLID C3D8R, SHELL S4R and SHELL S4R were selected to simulate concrete, adhesive and FRP sheet, respectively. The mesh size is around 0.01mm.

Table 1 Material properties of the FRP laminae and substrate concrete

	Young's modulus (GPa)	Density (kg/m ³)	Poisson's ratio
CFRP laminae	$E_{11} = 160$ $E_{22} = E_{33} = 8.6$	2000	$\nu_{12} = \nu_{13} = 0.011$ $\nu_{23} = 0.25$
Substrate concrete	$E = 30$	2500	0.2

It was assumed that the interfacial debonding occurred at the adhesive layer. The connection between adhesive layer and the concrete slab, and the connection between FRP layer and adhesive layer were both handled by TIE constraint. The boundary condition at the bottom of the concrete slab was defined as fixed end. The dynamic implicit algorithm was recommended as the computing method. The damping effect was assumed as Rayleigh damping, and the value of damping coefficient was determined according to frequency at the first two orders. The sinusoidal signal with a single frequency was adopted to simulate acoustic wave excitation. The linear chirp change of the acoustic wave was realized by changing the value of the frequency of this sinusoidal signal. The effect of the noise was considered by adding the white noise signal to the sinusoidal drive signal and the amplitude of white noise signal was one-tenth of that of sinusoidal signal. The finite element model of FRP-retrofitted concrete panel with an interfacial circular-shaped debonding damage is shown in Figure 2, where four red points in the figure from left to right were denoted as the excitation point of the focused sound beam, Point 1 at the debonding-free position along the FRP plate, Point 2 above the debonding damage along the FRP plate, and Point 3 at the debonding-free position along the FRP plate, respectively.

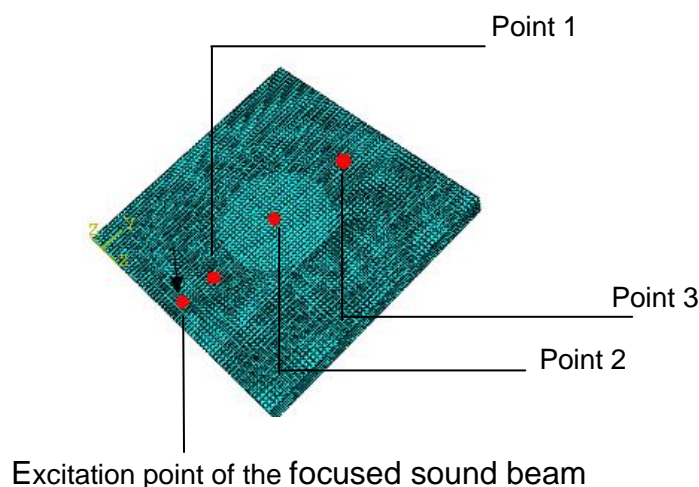


Figure 2 The finite element model with round-shape debonding

3.2 Feasibility Analysis

Feasibility analysis for this novel detection method was carried out by observing local vibration anomalies at the target surfaces (i.e. the four red points in Figure 2) under three loading configurations: 1) acoustic excitation at the resonant frequency relating to the debonding geometry on intact FRP-retrofitted panel (denoted as the case of Resonant & perfect); 2) acoustic excitation at the resonant frequency relating

to the debonding geometry on FRP-retrofitted panel with debonding damage (denoted as the case of Resonant & defective); and 3) acoustic excitation at the non-resonant frequencies relating to the debonding geometry on FRP-retrofitted panel with debonding damage (denoted as the case of Non-resonant). The result is shown in Figure 3. Distance (m) at x-axis refers to the distance measured from left edge of FRP along the FRP plate. The first peak for each curve refers to the location where the acoustic excitation applied. It can be observed from Figure 3 that the vibration amplitude for the point above the debonding damage along the FRP plate shows significant abnormality under the resonance excitation. Therefore, by measuring whether there is a large displacement amplitude increase of vertical vibration for the point on the thin plate under acoustic wave at certain resonant frequency relating to the defect geometry, the presence, location and size of debonding damage can be determined.

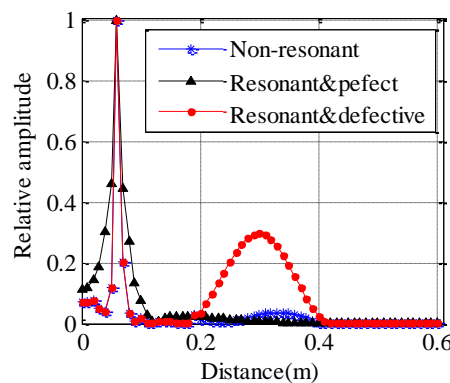


Figure 3 The vertical displacement amplitude along FRP surface

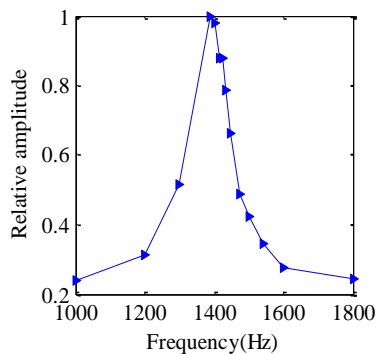
3.3 Relationship between vibration amplitude and excitation frequency

FRP-retrofitted panels and FRP-retrofitted beams under acoustic excitations with different resonant frequency values relating to different debonding geometry and size were calculated and the models and their natural vibration fundamental frequencies are shown in Table 2. As can be seen from Table 2, the natural vibration fundamental frequencies of FRP thin plate above the damage are all less than 2 KHz, and thus the acoustic waves can be simply generated by normal loudspeaker. The relationship between the excitation frequency and vibration amplitude of the point above the debonding damage along the FRP plate is shown in Figure 4.

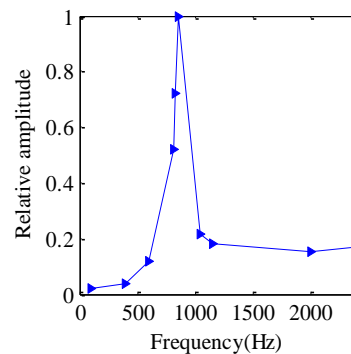
Table 2 Models of the FRP-retrofitted components with different types of debonding

Type of debonding	Size of debonding(diameter or side length) d/cm	Corresponding vibration at fundamental frequency/Hz
Circular-shape at mid-span of plate	6; 8; 10; 15; 20; 25	1390; 850; 560; 231; 130; 84
Circular-shape at mid-span of beam	10; 13; 15	550; 340; 240
Diamond-shape at mid-span of beam	6	1020
Rectangular-shape at the edge of beam	Short side: 6; long side: 8	115

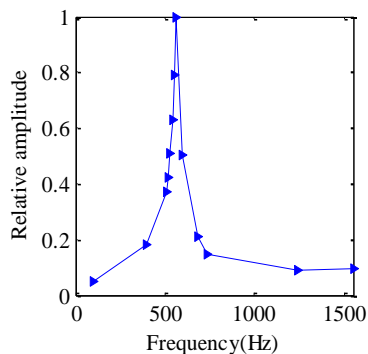
As shown in Figure 4, the relationship between the excitation frequency and relative vibration amplitude of the point above the debonding damage along the FRP plate shows the same pattern for FRP-retrofitted panels and FRP-retrofitted beams with different debonding geometry and size. When the excitation frequencies are far away from the resonance frequency, the relative vibration amplitudes of points are almost the same and the values of them are within 0.2. However, significantly higher relative vibration amplitude was observed at the resonant frequency relating to the defect geometry.



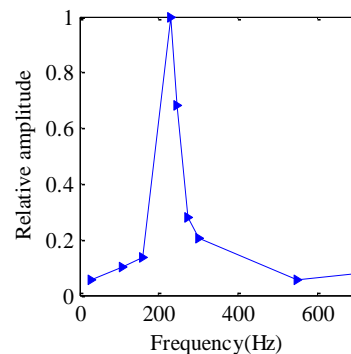
(a) Circle-shape debonding of plate d=6cm



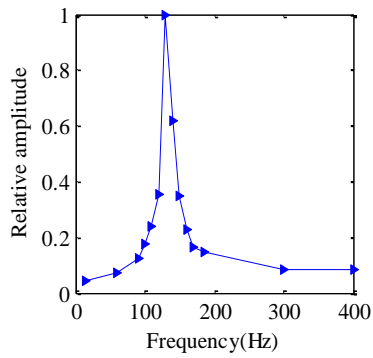
(b) Circle-shape debonding of plate d=8cm



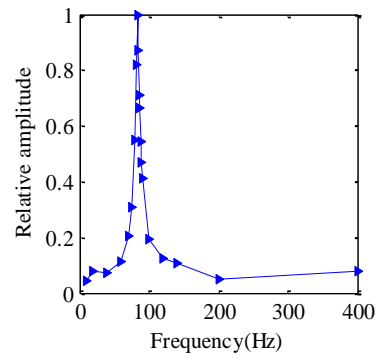
(c) Circle-shape debonding of plate d=10cm



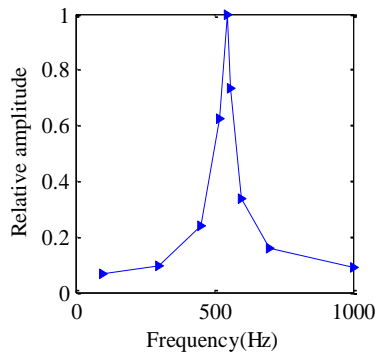
(d) Circle-shape debonding of plate d=15cm



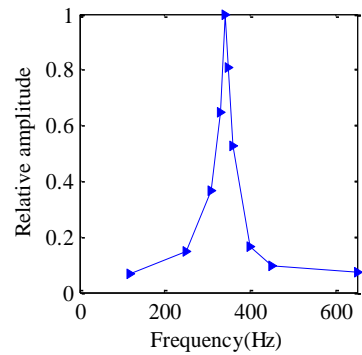
(e) Circle-shape debonding of plate d=20cm



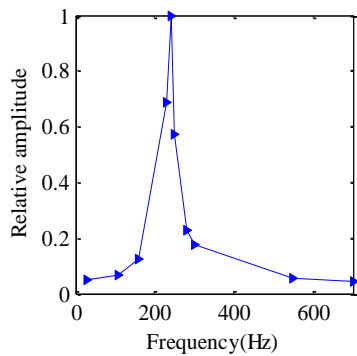
(f) Circle-shape debonding of plate d=25cm



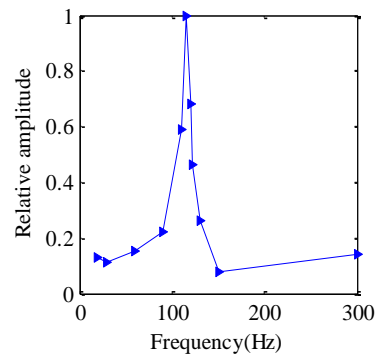
(g) Circle-shape debonding of beam d=10cm



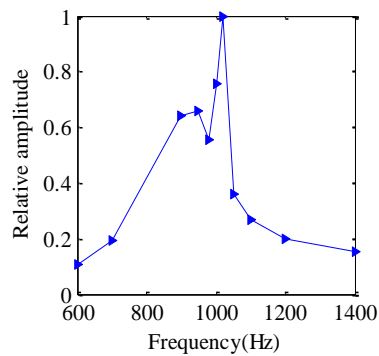
(h) Circle-shape debonding of beam d=13cm



(i) Circle-shape debonding of beam d=15cm



(j) rectangular-shape debonding of beam



(k) Diamond-shape debonding of beam

Figure4 The relationship between the vertical displacement relative amplitude and the excitation frequency

A FRP-retrofitted panel with a circular-shaped debonding (debonding diameter $d = 20\text{cm}$) has been selected in order to investigate the vibration amplitude difference for the point above the debonding damage and the points at the debonding-free positions along the FRP plate under different excitation frequencies. Figure 5 shows the locations for points at debonding-free positions along the FRP plate. The arrow denotes the location of acoustic excitation and the 4 dots denotes the locations for points from point 1 to point 4. The relationship between the excitation frequency and vibration amplitudes of points at the debonding-free positions along the FRP plate is shown in Figure 6. As shown in Figure 6, the vibration amplitudes of points at the debonding-free positions along the FRP plate under different excitation frequencies are almost the same. In other words, the vibration amplitudes of points at the debonding-free positions along the FRP plate do not vary with the excitation frequency change, which is essentially different from relationship between the excitation frequency and vibration amplitude of the point above the debonding damage along the FRP plate.

3.4 Numerical Simulation for point-by-point excitation method

The previous modeling method assumed that the location for the acoustic wave excitation point was invariable and the vibration anomalies for each point at the target surfaces can be measured with the high-sensitivity fiber optic interferometer. In this section, the locations of acoustic excitation point and measuring point at target surfaces changes simultaneously, i.e. the location of acoustic excitation moves along the length direction of the FRP plate point-by-point and the measuring point is always next to the location of acoustic excitation (Figure 7). The schematic diagram for point-by-point excitation method and fixed-point excitation method is shown in Figure 7. The vibration amplitudes of points along the FRP plate under both resonant excitation and non-resonant excitation have been calculated and compared by adapting point-by-point excitation method. Figure 8 shows the data of vibration amplitudes of points (the corresponding point next to the acoustic excitation position) along the FRP plate at acoustic excitation position for FRP-retrofitting panels with 10cm circular shape debonding and 15cm circular shape debonding, respectively. In Figure 8 the arrowed line denoted by W shows the actual extent of the interfacial debonding.

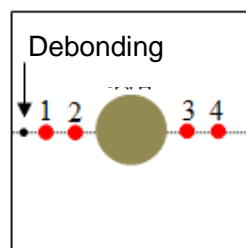


Figure 5 The location of observation points in debonding-free area

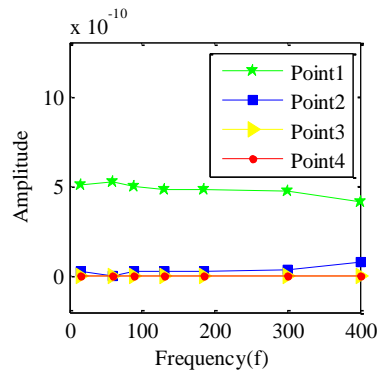


Figure 6 The relationship between the amplitude and the frequency (intact area)

As shown in Figure 8, when the acoustic excitation locates above the debonding damage area along the FRP plate, the vibration amplitude of the point always increases significantly regardless of resonant excitation or non-resonant excitation. However, the magnitude of the vibration amplitude of the point under resonant excitation is 20~40 times larger than the magnitude of amplitude under non-resonant excitation. Therefore, this point-by-point excitation method can detect the debonding damage location and extent more precisely than the fixed excitation location method, especially when the frequency of acoustic excitation is close to or equal to the fundamental natural frequency of the thin FRP plate located above the debonding damage. However, the acoustic excitation location has to be moved point by point along the FRP plate.

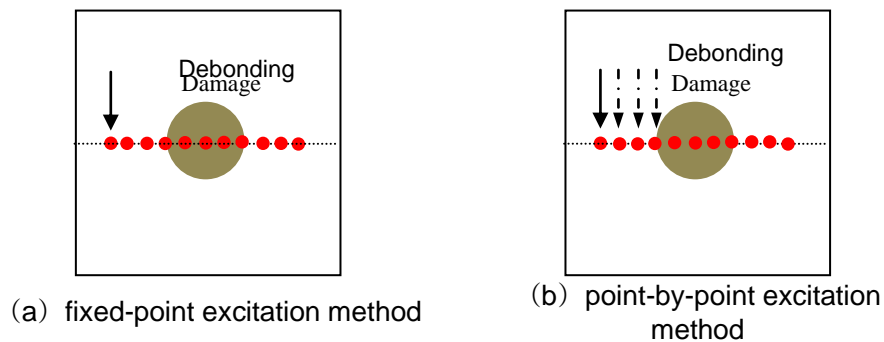


Figure 7 comparison between two methods

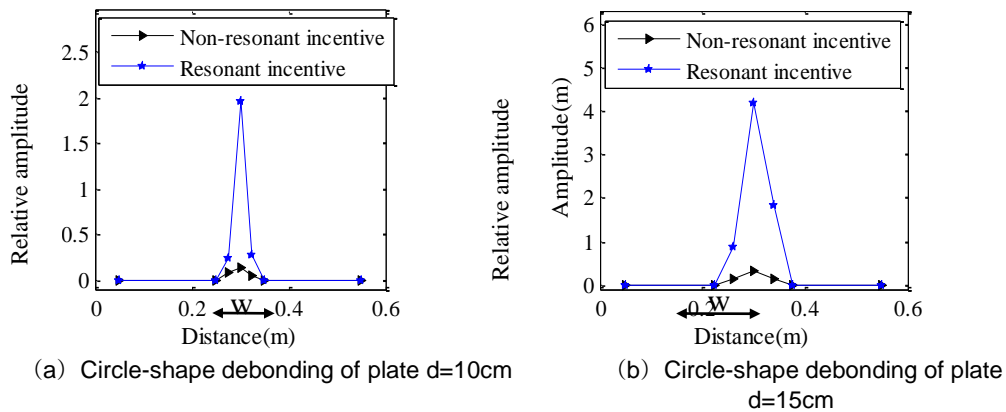


Figure 8 the results of the point-by-point excitation method

4. Experimental Investigation

4.1. Testing Specimen preparation

To demonstrate the feasibility of the technique, experimental testing of bonded repairs with interfacial debonding has been carried out on concrete panels and beams. Manufacturing procedure of FRP-retrofitted concrete panel specimens with artificial debonding damage is shown in Figure 9.

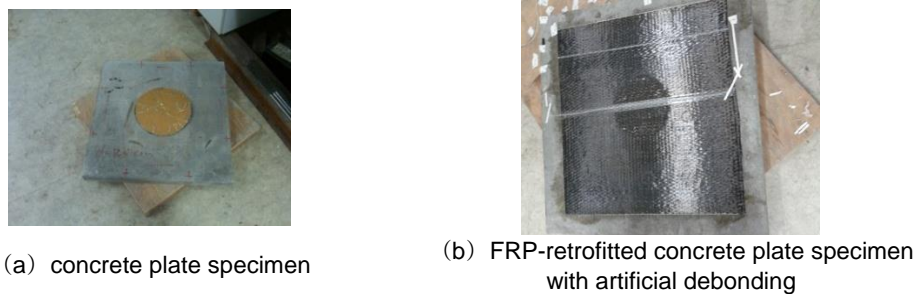


Figure 9 FRP reinforced concrete slab specimen with debonding

The geometry of concrete substrate is 600 mm*600 mm*40 mm. After the completion of the pouring of concrete panel, different sizes of rounded plastic sheets with 1mm in thickness was put on the concrete panel at the specified location to produce rounded groove on its surface (Figure 9(a)). The interfacial circular-shape debonding was thus produced by this groove which separated CFRP sheets and concrete substrate. The diameters of artificial debonding for each FRP-retrofitted concrete panel are 10cm, 15cm, 20cm, 25cm, respectively. Two layers of CFRP sheets were then brushed on the surface of concrete by hand lay-up of 2 plies of

lamina (each ply with a thickness of 0.11 mm) along the same orientation, followed by curing under normal temperature (Figure 9(b)). During the lay-up, the edge of each sheet has to be carefully aligned and epoxy is uniformly brushed onto the sheet. Pressure is applied through a small roller to avoid the formation of resin-rich regions or air bubbles.

4.2. Experimental Set-up

The experimental schematic layout for interfacial debonding detection of CFRP-retrofitting concrete substrates (i.e., concrete panels or beams) with acoustic-optic technique is shown schematically in Figure 10. Since the fundamental natural frequencies of the thin FRP plates located above the debonding zone are all within the range of audible sound waves in this paper, a loudspeaker which drives a linear chirp is adopted to generate focused acoustic beam such that the beam diameter can be controlled to directly and locally excite the surface area where damages/defects are embedded in the FRP-concrete systems. A pre-attached high-sensitivity fiber optic interferometer is used to detect the local micro vibration of the FRP reinforced structure surface caused by the acoustic excitation. By comparing the local vibration amplitudes at the surface above the debonding damage position to the surfaces above debonding-free positions along the FRP plate, the interfacial debonding can be detected, mapped, and quantified according to the measured vibration anomalies at the target surface. The feasibility and the numerical analysis of this technique can then be verified. The frequency range of ambient noise in the lab are mostly within the low frequency range ($\cong 10\text{Hz}$) and the magnitude of the noise is very small. However, the frequency range of the loudspeaker is from 50 Hz to 2000Hz. Therefore, the ambient noise can be substantially eliminated through filtering. The detailed experiment set-up according to schematic layout is shown in Figure 11.

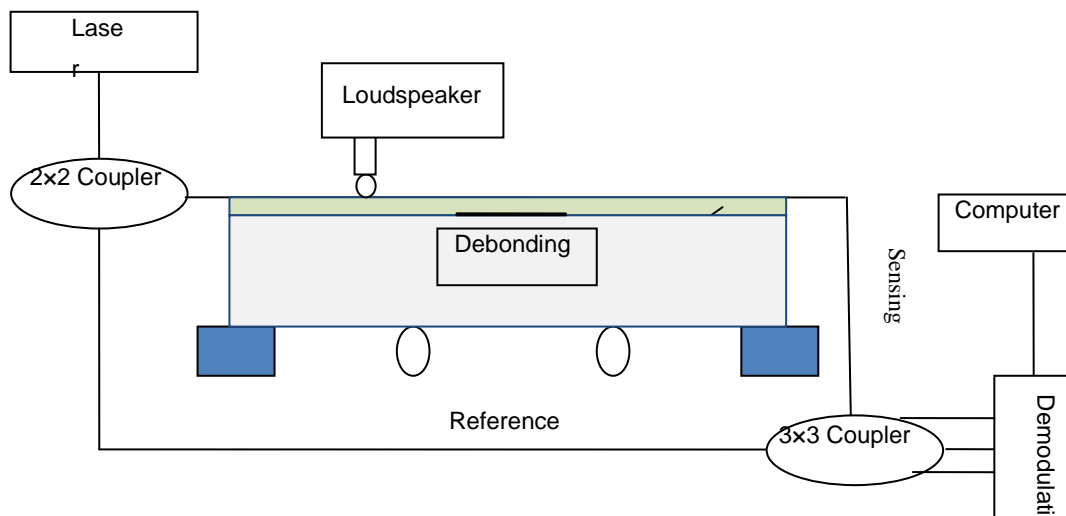


Figure10 The schematic layout of experimental system

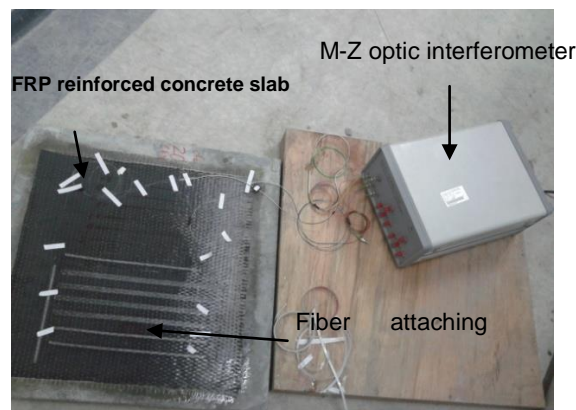


Figure 11 The detailed experiment set-up

The loudspeaker is located above the FRP-retrofitted concrete panel to generate acoustic waves excitation with linear frequency conversion. Both fixed-point excitation method and point-by-point excitation method were investigated during the experimental work. According to acoustic excitation range of loudspeaker, the sampling frequency of fiber optic interferometer is determined as 6 kHz. The sensing beam of M-Z fiber optic interferometer is attached at different target positions from surfaces above debonding-free area to surface above debonding damage zone discretely. The results from the M-Z fiber optic interferometer at each target surface were processed through MATLAB to obtain the corresponding vibration amplitudes under various acoustic excitation frequencies.

4.3 Results and Discussions

Figure 12 shows both the numerical result and experimental result of the vibration

amplitude of the point above the debonding damage along the FRP plate vs. excitation frequency for FRP-retrofitting panels with 20cm circular shape debonding and 25cm circular shape debonding, respectively.

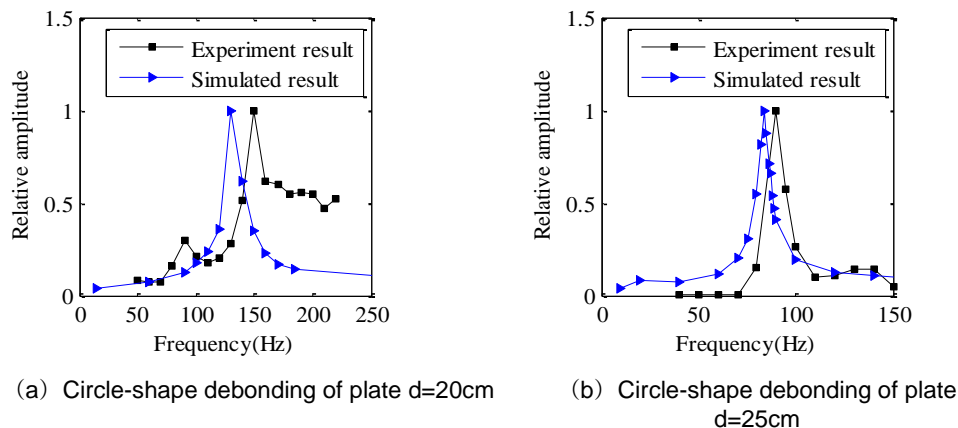
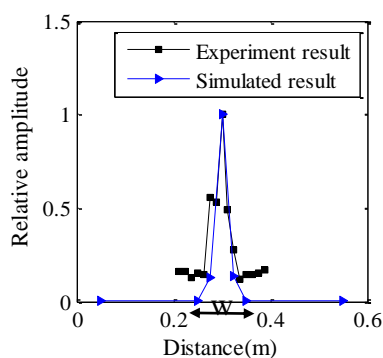


Figure 12 Relationship between vertical vibration displacement amplitude and excitation frequency of thin plate over the debondings

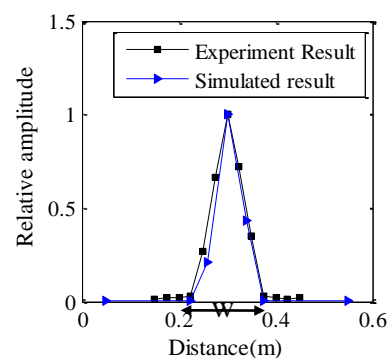
The focused acoustic waves were applied on the FRP plate through fixed-point excitation method. As shown in Figure 12, the experimental result is quite close to numerical result while vibration amplitude of the point above the debonding damage changes with the change of excitation frequency. In each figure the arrowed line denoted by W shows the actual extent of the interfacial debonding. When the excitation frequency is close or equal to the natural frequency of the thin FRP plate located above the debonding damage, the magnitude of vibration amplitude of the point above the debonding damage increases about 3~4 times. By observing significant high velocity measurements at the debonding location and at the resonant frequency relating to the defect geometry, the presence, location and extent of the debonding damage can be deduced. It can be seen from Figure 12 that there is a dozen Hz deviation at peak value of frequency for experimental result and numerical result. This deviation may be due to the manufacturing error of artificial debonding damage shape or diameter during the curing process in the lab, which cause the deviation of natural frequency peak value for thin FRP plate. It should be noted that the integral strain values in this case is very small (less than 1 μ m) due to the power limit of the loudspeaker. Small errors induced by, for example, variations in the elastic support, can lead to relatively large changes in the integral strain curve, which shows up as additional peaks and troughs (Figure 12(a)). Despite the presence of these additional features, the effect of debonding can still be clearly revealed in the

experimental data, although the peak location may not match exactly with the debonding diameter.

Figure 13 shows both the numerical result and experimental result of the vibration amplitudes of points along the FRP plate vs. acoustic excitation position for FRP-retrofitted panels with 10cm circular shape debonding and 15cm circular shape debonding, respectively. The focused acoustic waves were applied on the FRP plate through point-by-point excitation method and the acoustic excitation frequency is the resonance frequency which equal to the natural frequency of the thin FRP plate located above the debonding damage. As shown in Figure 13, the experiment result is very close to numerical result. When the acoustic excitation locates above debonding-free positions along the FRP plate, the vibration amplitudes of the points (the corresponding points next to the acoustic excitation positions) along the FRP plate is very close to each other and the value of them are relatively small. However, when the acoustic excitation moves to the location above debonding damage area along the FRP plate, the vibration amplitude of point is increased by dozens of times. In other words, when the acoustic excitation moves to the edge between debonding-free area and debonding area (including left and right edge of the debonding zone), a sudden “jump” of the vibration amplitude (or a sudden increase in slope of the vibration amplitude versus excitation position curve) is observed. The debonding location and extent can be determined by observing the sudden increase in slope of the curve. When the acoustic excitation continues to move into debonding-free location, the curve becomes gentle again while the amplitude begins to decrease by times.



(a) Circle-shape debonding of plate $d=10\text{cm}$



(b) Circle-shape debonding of plate $d=15\text{cm}$

Figure 13 Comparison between the experimental results and numerical simulation through by-point test under resonant frequency

4. Conclusion

(1)Based on the results from both numerical and experimental studies, the feasibility of interfacial debonding detection in FRP-retrofitted Structures with acoustic-optic nondestructive detection technique is demonstrated. The acoustic waves with linear frequency conversion can be generated through a loudspeaker which drives a linear chirp and the vibration anomalies can be measured at the target surface using a pre-attached high-sensitivity fiber optic interferometer. The result shows that the presence, location and extent of the debonding damage can be deduced by observing significant high velocity measurements at the debonding location and at the resonant frequency relating to the defect geometry.

(2)Feasibility analysis for this novel detection method was carried out by numerical analysis for local vibration anomalies at the target surfaces for intact FRP-retrofitting concrete structures, and FRP-retrofitting panels and FRP-retrofitted beams with different debonding geometries and sizes. The relationship between vibration amplitude of the points above the debonding damage along the FRP plate and excitation frequency has been studied in detail and significant abnormality of vibration amplitude for the point above the debonding damage along the FRP plate can be observed under the resonance excitation.

(3)By comparison of both numerical results and experimental results for fixed-point excitation method and point-by-point excitation method of this technique, it was found that the point-by-point excitation method can detect the debonding damage location and extent more precisely than the fixed excitation location method, especially when the frequency of acoustic excitation is close to or equal to the fundamental natural frequency of the thin FRP plate located above the debonding damage. However, the acoustic excitation location has to be moved point by point along the FRP plate

Acknowledgement

This work is supported by the funding of NSFC (51278156).

Reference

- Taljsten B. (1997), "Strengthening of beams by plate bonding", J Mat. Civ Eng, ASCE,9(4),206–12.
- Hollaway L C. (2010), "A review of the present and future utilisation of FRP composites in the civil infrastructure with reference to their important in-service properties[J]", Construction and Building Materials, 24(12),2419-2445.
- Schmachtenberg E, Schulte Zur Heide J, Töpker J.(2005), "Application of ultrasonics for the process control of Resin Transfer Moulding (RTM)[J] ", Polymer Testing, 24(3),330-338.

- Bastianini F, Di Tommaso A, Pascale G.(2001), "Ultrasonic non-destructive assessment of bonding defects in composite structural strengthenings[J]", *Composite Structures*, 53(4),463-467.
- Galea SG, et al.(2001), "Overview of DSTO smart structures activities related to structural health monitoring",HUMS 2001-DSTO international conference on health and usage monitoring.
- Cao G H , Fang Z, Wu J F. (2005), "Experimental study on continuous RC beams strengthened with FRP laminates[J]",*Building Structure*, (10),63-66.
- Hart-Smith LJ.(1982), AFWAL-TR-82-4172.
- Shahawy M.(1995), "Strengthening highway bridges with carbon fiber materials",74th Annual meeting of the transportation research board, Washington (DC).
- Gibson,Ronald F.(1994), *Principles of composite material mechanics [M]*, international editions , McGraw-Hill book Co., section 7.8.
- Meier U, Deuring M, Meier H, Schwegler G.(1992),"Strengthening of structures with CFRP laminates: research and applications in Switzerland", Neale KW, Labossiere P, editors. *Advanced composite materials in bridges and structures*. Montreal (PQ),CSCE, 243–51.
- Neale KW, Laboissiere P.(1997), "State-of-the-art report on retrofitting and strengthening by continuous fiber",*Canada Non-metallic (FRP) reinforcement for concrete structures*, Japan Concrete Institute, 1,25–40.
- Liu H X,Zhang H, Ma R X.(2003), "Nondestructive testing techniques for composite materials[J]", *Nondestructive Testing and Evaluation International*, 631-634.
- Chen M X, Fang Z.(2004), "Study on application of fiber reinforced plastic in civil engineering[C]", *Bridge the Sixteenth National Conference Proceed*, Changsha, China.
- Leung CKY.(2001), "Delamination failure in concrete beams retrofitted with a bonded plate", *J Mater Civ Eng* ,13(2),106–13.
- Huang P Y, Zhou X P, Zhao C.(2002), "Some key mechanical Problems on FRP sheet applied in civil engineering[J] ", *Journal of South China University of Technology (Natural Science Edition)*, 101-105.